Robust updating of uncertain damping models in structural dynamics for low- and medium-frequency ranges

Evangéline Capiez-Lernout, Christian Soize

Robust updating of uncertain damping models in structural dynamics for low- and medium-frequency ranges.

Capiez-Lernout, E.[1,⋆], Soize,C. [2]

[1] Evangeline.Capiez-Lernout@univ-mlv.fr

[2] Christian.Soize@univ-mlv.fr

Laboratoire de Mecanique

Universite Paris-Est

Laboratoire de Mecanique (LaM)

EA 2545

5, Boulevard Descartes,

77454 Marne la Vallee, Cedex 02, France

Tel: 00 33 1 60 95 77 98

Fax: 00 33 1 60 95 77 99.

⋆ *Corresponding author.*

Preprint submitted to Mechanical Systems and Signal Processing *14 November 2007*

Abstract

This paper deals with the robust updating of uncertain computational models in the context of structural dynamics in the low- and medium-frequency ranges of composite sandwich panels for which experimental results are available. The uncertain computational model is constructed using the non-parametric probabilistic approach which takes into account model and data uncertainties. The formulation of the robust updating problem includes the effects of uncertainties and consists in minimizing a cost function with respect to an admissible set of updating parameters. Updating is performed in two steps using several cost functions and experimental results. The results of the robust updating problem show that the method proposed is efficient for updating the uncertain computational model in both low- and medium-frequency ranges.

Key words: Robust updating, Structural dynamics, Model uncertainties, Composite sandwich materials, Low-frequency range, Medium-frequency range.

1 Introduction

In structural dynamics, the updating of a computational model using experimental data is currently a challenge of interest in many industrial areas. It is known that the dynamical behaviour of a real structure manufactured from a designed structure has to be predicted with a computational model constructed with a probabilistic model in order to take into account the model uncertainties and the data uncertainties. Consequently, the updating has to be carried out with an uncertain computational model, which allows the effects of uncertainties in the updating process to be taken into account. Such an updating is understood as robust updating. Note that

the quality of the robust updating is conditioned by the probability model used for constructing the uncertain computational model. In general, the updating process is performed with a deterministic computational model [1–10].

More recently, robust updating formulations have been proposed in the context of structural dynamics [11–15]. Such robust updating formulations concern the robust updating with respect to data uncertainties. This means that the uncertain computational model which has to be updated is constructed with a parametric probabilistic approach. In such a case, the parameters of the mean computational model are modelled by random variables or stochastic fields in order to take into account the data uncertainties. Note that such an uncertain computational model does not take into account the model uncertainties. Consequently, the mean computational model has to model the structural complexity of the dynamical system with a high accuracy in order to be predictive. This means, that the more complex the dynamical system is, the larger the number of parameters is.

The motivation of this paper is to propose a robust updating methodology with respect to both model uncertainties and data uncertainties in the low- and medium-frequency ranges using experimental measurements. Concerning the present robust optimization approach, it should be noted that, to the knowledge of the authors, there is a prior work carried out in that sense in the field of robust design optimization [16,17] but none in the present context of robust updating optimization. The present robust udating optimization is briefly summarized as follows. The uncertain computational model which has to be updated is constructed with the non-parametric probabilistic approach [18,19] whose relevance and efficiency has been proven in structural dynamics [20–23] and in structural acoustics [24,25]. The main idea of this approach is to avoid

a complex modelling of the mean computational model. A set of mean computational models whose design parameters are called the updating mean parameters and belong to an admissible set defined by the design constraints is constructed. This mean computational model has to be representative of the physics of the problem although it remains a rough approximation of the dynamical system. Consequently, it should be noted that the admissible set of the updating mean parameters has a reasonable dimension. The non-parametric probabilistic model is then used to take into account model uncertainties and data uncertainties. The operators of the mean computational model are replaced by random operators whose probability model is constructed from the maximum entropy principle with the available information. With such an approach, the uncertainty level of each random operator is controlled by a scalar parameter called the dispersion parameter. This non-parametric probabilistic approach allows not only the data uncertainties (uncertainties on the parameters of the mean computational model) to be taken into account but also the model uncertainties (uncertainties due to the lack of accuracy in the mean computational model). One then obtains a set of uncertain computational models whose updating parameters are the updating mean parameters related to the mean computational model and the updating dispersion parameters which allow the uncertainty level in the computational model to be controlled. The cost function used for the robust updating is defined as a function of these updating parameters and is the sum of the normalized variance of the dynamical response of the stochastic computational model and of the bias defined as the distance between the mean stochastic response and the mean of the experimentally measured response.

The robust updating leads a non-linear constrained optimization problem to be solved with respect to the admissible set of the updating parameters. The robust updating methodology is splitted in two steps. The first step consists in calculating the initial updating parameters. First,

the initial updating mean parameters are deduced from deterministic updating, that is to say by using a cost function constructed from the mean computational model and defined as a distance between the mean computational model and the mean of the experiments. It is known that the information contained in the unwrapped phase of a frequency response function is interesting (see for instance [26–28]) although rarely used for the analysis of mechanical systems. One proposes then to solve this deterministic updating by using two cost functions. The first one is defined from the modulus of the frequency response functions (usual method). The second one is a new approach which uses the unwrapped phase of the frequency response functions. The efficiency of these two cost functions is then compared and discussed. Secondly, the initial updating dispersion parameters are deduced by using the cost function defined for the robust updating and previously constructed from the uncertain computational model for which the updating mean parameters are set to their initial value. The second step consists then in solving the robust updating optimization problem around the initial updating parameters. The methodology is validated and compared in the context of the structural dynamics of composite sandwich panels in the low- and medium-frequency ranges for which experimental results issued from a set of 8 manufactured sandwich panels are available [23,25].

In Section 2, the experimental results are summarized. Section 3 is devoted to the deterministic updating of the mean computational model in order to calculate the initial updating mean parameters. In Section 4, one proposes the construction of a cost function in order to formulate the robust updating problem with respect to model and data uncertainties. This cost function is then used (1) for calculating the initial updating dispersion parameters and (2) for solving the robust updating optimization problem around the initial updating parameters. The methodology is numerically validated from experiments.

2 Experiments in the low- and medium- frequency ranges

2.1 Description of the experimental data

Experimental data related to a set of $n_{exp} = 8$ multilayered sandwich panels manufactured from a designed composite sandwich panel [23,25] is used. The designed composite sandwich panel is a free structure with rectangular shape and is made up of two thin carbon-resin skins constituted of two unidirectional plies [60/-60] and of one high stiffness closed-cell foam core. Dynamical experiments are conducted for each of the manufactured sandwich panels. The detailed description of the designed sandwich panel and of its corresponding experimental protocol can be found in [23,25]. Figure 1 displays several samples of the sandwich panel. The frequency response function corresponding to a given out-plane point load is measured at $n_{obs} = 24$ observation points in the frequency band of analysis $\mathbb{B} = [100\,,\,4500]\,Hz$. Let $\mathbf{x}_j$ with $j \in \{1, \ldots, n_{obs}\}$ be the location of the observation point number j. One denotes by $W_j^{exp}(\omega, \theta_k)$ the observation corresponding to the experimental frequency response function of the manufactured composite sandwich panel number k, measured at observation point $\mathbf{x}_j$, at a given frequency $\nu = \dfrac{\omega}{2\,\pi}$ of frequency band $\mathbb{B}$ and expressed in terms of acceleration.

2.2 Analysis of the experimental results

When analyzing linear dynamical systems in the frequency domain, the frequency response functions are complex. Most often, the dynamic analyses are carried out with the moduli of the frequency response functions and the information provided by the phases of frequency re-

sponse functions is usually not investigated. It is known that the phase of a frequency response function is able to characterize the different frequency ranges of analysis (low-frequency range, medium-frequency range, high-frequency range) [29]. In the low-frequency range, for which there is a low modal density, there are rotations of the phase each time an isolated mode is crossed. Representing the phase as an unwrapped phase yields an unwrapped phase which is a non-monotoneous function of the frequency, for which the rotations of the phase are represented by discontinuities. In the high-frequency range, for which there is a high modal density, the modes are overlapped and there is no rotation of the phase. Consequently, the unwrapped phase is a linear mapping of the frequency. The medium-frequency range is characterized by an unwrapped phase which is not linear but which is a smooth function of the frequency. Consequently, since the information provided by the phase is rich and is usually not often used in linear dynamics for updating optimization, one proposes to analyze the experimental data not only from the moduli of the experimental frequency responses (usual approach) but also from the phases of the experimental frequency response functions.

The experimental complex-valued frequency response function $W_j^{exp}(\omega, \theta_k)$ can be written as $W_j^{exp}(\omega, \theta_k) \, = \, |W_j^{exp}(\omega, \theta_k)| \exp(-i \, \Phi_j^{exp}(\omega, \theta_k))$ in which $|W_j^{exp}(\omega, \theta_k)|$ and $\Phi_j^{exp}(\omega, \theta_k)$ are the modulus and the unwrapped phase angle. In order to analyze the experimental data, the following quantities corresponding to a spatial average of moduli and of unwrapped phases are introduced as:

$$\underline{dB}_w^{exp}(\omega) \, = \, 10 \, \log_{10} \left(\frac{1}{n_{obs} \, n_{exp}} \sum_{k=1}^{n_{exp}} \left(\sum_{j=1}^{n_{obs}} |W_j^{exp}(\omega, \theta_k)|^2 \right) \right) \quad , \tag{1}$$

$$\underline{\phi}_w^{exp}(\omega) \, = \, \frac{1}{n_{obs} \, n_{exp}} \sum_{k=1}^{n_{exp}} \sum_{j=1}^{n_{obs}} \Phi_j^{exp}(\omega, \theta_k) \quad , \tag{2}$$

Figure 2 displays the graph $\nu \mapsto \underline{dB}_w^{exp}(\nu)$ where $\nu \, = \, \omega / (2 \, \pi)$ is the frequency in Hz. Figure 3

displays the graph $\nu \mapsto \underline{\phi}_w^{exp}(\nu)$. In Figure 3, it should be noted that the low-frequency range and the medium-frequency range can be easily identified from each other. The low-frequency range is characterized by the low-frequency band $\mathbb{B}_L$ for which $\underline{\phi}_w^{exp}(\nu)$ is a non-monotoneus function of the frequency ν, showing discontinuities when crossing an isolated resonance. Analyzing Figure 3 (but also Figure 2) yields $\mathbb{B}_L = [100\,,\,1200]\,Hz$. As the frequency grows, the modal density increases and the medium-frequency range corresponds to the medium-frequency band $\mathbb{B}_M$ for which $\underline{\phi}_w^{exp}(\nu)$ is a smooth function of ν. In Figure 3, it can be seen that $\mathbb{B}_M = [1200\,,\,4500]\,Hz$.

3 Updating method for the mean computational model of the dynamical system using the experimental frequency response functions

3.1 Motivation and strategy

The mean computational model related to the designed sandwich panel is constructed by the finite element method. In this Section, one investigates a deterministic updating method in order to update the mean computational model using experimental measurments. Such an updating method has to be efficient both in the low-frequency range and in the medium-frequency range. It is assumed that the conservative part (mass and stiffness) has already been updated [23]. In this paper, one proposes to update the damping model in the low- and medium-frequency ranges. In general, damping depends on the frequency in the medium-frequency range. Consequently, the damping model used has to take into account this dependance with the frequency. A damping model controlled by four updating mean parameters defined on a given admissible

set of updating mean parameters is introduced. The mean computational model is then updated with respect to this admissible set using the experimental data. First, a usual updating method consisting in minimizing the cost function defined as a distance between a spatial average of moduli of the frequency response functions and the corresponding experimental data is used. Secondly, based on the information contained in the unwrapped phase of a given frequency response function, one proposes a new approach consisting in using a spatial average of the unwrapped phase of the frequency response functions in order to construct a cost function.

3.2 Description of the mean finite element model

The mean finite element model of the designed sandwich panel which has to be updated is a laminated composite thin plate in bending mode. Its middle plane occupies the domain $[0\,,\,0.4] \times [0\,,\,0.3]\,m$ in the plane (Ox, Oy) of a cartesian coordinate system $(O\,x\,y\,z)$. The out-plane displacements are only considered. The laminated composite thin plate is constituted of five layers, each one made up of an orthotropic elastic material. The first two layers are two unidirectional plies in a $[-60/60]$ layup with width $0.00017\,m$, mass density $1600\,kg.m^{-3}$ and whose elasticity constants expressed in the local coordinate system $(O\,X\,Y\,z)$ are given by $E_X = 101\,GPa$, $E_Y = 6.2\,GPa$, $\nu_{XY} = 0.32$, $G_{XY} = G_{XZ} = G_{YZ} = 2.4\,GPa$. The third layer is a closed-cell foam with thickness $0.01\,m$, mass density $80\,Kg.m^{-3}$ and elasticity constants $E_x = E_y = 60\,MPa$, $\nu_{xy} = 0$, $G_{xy} = G_{xz} = G_{yz} = 30\,MPa$. The last two layers are two unidirectional plies in a $[60/-60]$ lay-up with the same characteristic as the first two layers. The laminated thin plate is a free structure. The finite element mesh is constituted of 64×64 rectangular four nodes elements and has $n = 12\,288$ DOF. Figure 4 shows the

corresponding finite element mesh. The mean finite element model is submitted to a deterministic unit transverse load constant in frequency band $\mathbb{B}$ with amplitude 1 and located at the node with coordinates $(0.187, 0.103, 0)$. In the present case, the updating concerns the model used for modeling the damping in the composite panel. Let $\mathbf{r}$ be the vector of the updating parameters. Vector $\mathbf{r}$ belongs to an admissible set $\mathcal{R}$ corresponding to a given family of damping models that is defined in the next Subsection. Assuming the designed sandwich panel to be linear and slightly damped, for fixed $\mathbf{r}$ belonging to $\mathcal{R}$ and for fixed ω belonging to $\mathbb{B}$, the mean finite element matrix equation of the sandwich panel is written as

$$(-\omega^2\,[\underline{M}] \,+\, i\,\omega\,[\underline{D}(\mathbf{r})] \,+\, [\underline{K}])\,\underline{\mathbf{u}}(\mathbf{r},\omega) \,=\, \underline{\mathbf{f}}(\omega) \quad , \tag{3}$$

in which $\underline{\mathbf{u}}(\mathbf{r},\omega)$ is the $\mathbb{C}^n$-vector of the n DOF and where $\underline{\mathbf{f}}(\omega)$ is the $\mathbb{C}^n$-vector induced by the external forces. Since the sandwich panel has a free boundary, the mean mass matrix $[\underline{M}]$ is a positive-definite symmetric $(n \times n)$ real matrix and the mean damping and stiffness matrices $[\underline{D}(\mathbf{r})]$ and $[\underline{K}]$ are positive semi-definite symmetric $(n \times n)$ real matrices. It should be noted that the rank of mean matrices $[\underline{D}(\mathbf{r})]$ and $[\underline{K}]$ is $n-3$ (presence of three rigid body modes). For j belonging to $\{1,\ldots,n_{obs}\}$, the frequency response functions expressed in terms of acceleration at point $\mathbf{x}_j$ are denoted by $\underline{w}_j(\mathbf{r},\omega)$ and are stored in the $\mathbb{C}^{n_{obs}}$-vector $\underline{\mathbf{w}}(\mathbf{r},\omega) \,=\, (\underline{w}_1(\mathbf{r},\omega),\ldots,\underline{w}_{n_{obs}}(\mathbf{r},\omega))$ such that $\underline{\mathbf{w}}(\mathbf{r},\omega) \,=\, [T(\omega)]\,\underline{\mathbf{u}}(\mathbf{r},\omega)$, in which $[T(\omega)]$ is the $(n_{obs} \times n)$ observation matrix.

3.3 Description of the mean reduced matrix model

The mean reduced matrix model of the sandwich panel is constructed by modal analysis. Since we are interested in the elastic motion of the structure, we introduce the $(n \times N)$ real matrix $[\underline{\Phi}]$ whose columns are the $N \ll n$ eigenvectors $\underline{\boldsymbol{\varphi}}_j$ related to the N positive lowest eigenvalues $\underline{\lambda}_j = \underline{\omega}_j^2$. The mean reduced matrix model is then written as $\underline{\mathbf{w}}(\mathbf{r},\omega) = [T(\omega)]\,[\underline{\Phi}]\,\underline{\mathbf{q}}(\mathbf{r},\omega)$ in which $\underline{\mathbf{q}}(\mathbf{r},\omega)$ is the $\mathbb{C}^N$-vector of the generalized coordinates which is solution of the matrix equation

$$\Big(-\omega^2\,[\underline{\mathcal{M}}] + i\,\omega\,[\underline{\mathcal{D}}(\mathbf{r})] + [\underline{\mathcal{K}}] \Big)\,\underline{\mathbf{q}}(\mathbf{r},\omega) = \underline{\boldsymbol{\mathcal{F}}}(\omega) \tag{4}$$

In Eq. (4), the $\mathbb{C}^N$-vector $\underline{\boldsymbol{\mathcal{F}}}(\omega)$ is written as $\underline{\boldsymbol{\mathcal{F}}}(\omega) = [\underline{\Phi}]^T\,\underline{\mathbf{f}}(\omega)$ and the matrices $[\underline{\mathcal{M}}]$ and $[\underline{\mathcal{K}}]$ are the positive-definite symmetric $(N \times N)$ real diagonal matrices such that $[\underline{\mathcal{M}}]_{jk} = \mu_j\,\delta_{jk}$ and $[\underline{\mathcal{K}}]_{jk} = \underline{\mu}_j\,\underline{\omega}_j^2\,\delta_{jk}$ in which $\underline{\mu}_j$ is the generalized mass related to eigenmode $\underline{\boldsymbol{\varphi}}_j$ and where δ_{jk} denotes the Kronecker symbol. The mean reduced damping matrix $[\underline{\mathcal{D}}(\mathbf{r})]$ (which is a positive-definite symmetric $(N \times N)$ real matrix) is then introduced such that $[\underline{\mathcal{D}}(\mathbf{r})]_{jk} = 2\,\underline{\mu}_j\,\underline{\omega}_j\,\underline{\xi}_j(\mathbf{r})\,\delta_{jk}$ in which $\underline{\xi}_j(\mathbf{r})$ is the mean modal damping rate related to eigenmode $\underline{\boldsymbol{\varphi}}_j$ defined as $\underline{\xi}_j(\mathbf{r}) = f(\underline{\omega}_j,\mathbf{r})$. Let $\mathbf{r} = \{\xi_0,\xi_1,\alpha,\beta\}$ be the $\mathbb{C}^4$-vector of the updating mean parameters belonging to the admissible set $\mathcal{R}$ defined as $\mathcal{R} = \Big\{\{\xi_0,\xi_1,\alpha,\beta\}, \xi_1 \geq \xi_0 > 0; \alpha > 1; \beta > 0\Big\}$. For $\mathbf{r}$ fixed in $\mathcal{R}$, the function $b \mapsto f(b,\mathbf{r})$ is defined from $\mathbb{R}^+$ into $\mathbb{R}^+$ by

$$f(b,\mathbf{r}) = \xi_0 + (\xi_1 - \xi_0)\,\frac{b^\alpha}{b^\alpha + 10^\beta} \quad . \tag{5}$$

Its graph is displayed in Figure 5. It should be noted that admissible set $\mathcal{R}$ is defined in order that the family of functions $\{b \mapsto f(b,\mathbf{r})\}_{\mathbf{r}\in\mathcal{R}}$ has the following properties: for $\mathbf{r}$ fixed in $\mathcal{R}$, the function $b \mapsto f(b,\mathbf{r})$ is (1) a continuous increasing function from $\mathbb{R}^+$ into $[\xi_0\,,\,\xi_1]$; has (2) a zero

first derivative with respect to b in $b = 0$; has (3) an horizontal asymptote for $b \mapsto +\infty$; has (4) one inflection point whose position is controlled by parameters α and β. The algebraic representation of the damping rate which has been constructed uses the following properties. In such a dynamical system, the damping is approximatively constant in the frequency bands $[0\,,\omega_1]$ and $[\omega_2\,,+\infty[$ with $\omega_1 < \omega_2$. In the transition band $[\omega_1\,,\omega_2]$, the damping rate is increasing. The proposed model is a simple one corresponding to these properties. However, the use of such a simplified model induces model uncertainties and this is the reason why a probabilistic model of uncertainties is introduced for the generalized damping matrix. Consequently, the problem is not to only update a mean computational model but also to update the stochastic computational model as the predictive model. Finally, it should be noted that the robust updating methodology presented in this paper does not depend on the damping model used and can be applied to any damping models.

In a first step, one updates the mean computational model to get an initial value of the updating parameters and in a second step, one updates the stochastic computational model which is the predictive model.

3.4 Updating the mean computational model of the designed sandwich panel with experiments.

In this section, two formulations are proposed in order to update the mean computational model of the sandwich panel with the experiments. Similarly to Eqs. (1) and (2), the following obser-

vations are introduced

$$\underline{dB}_w(\mathbf{r},\omega) \;=\; 10\,\log_{10}\left(\frac{1}{n_{obs}}\,\left(\sum_{j=1}^{n_{obs}}|\underline{w}_j(\mathbf{r},\omega)|^2\right)\right) \quad , \tag{6}$$

$$\underline{\phi}_w(\mathbf{r},\omega) \;=\; \frac{1}{n_{obs}}\sum_{j=1}^{n_{obs}}\underline{\phi}_j(\mathbf{r},\omega) \quad , \tag{7}$$

in which $|\underline{w}_j(\mathbf{r},\omega)|$ and $\underline{\phi}_j(\mathbf{r},\omega)$ are the modulus and the unwrapped phase angle of $\underline{w}_j(\mathbf{r},\omega)$. Two formulations are then proposed in order to update the mean computational model of the sandwich panel with respect to updating mean parameter $\mathbf{r}$. The first cost function is written as

$$\underline{j}_{mod}(\mathbf{r}) \;=\; \frac{||\underline{dB}_w(\mathbf{r},.) \;-\; \underline{dB}_w^{exp}||_{\mathbb{B}}^2}{||\underline{dB}_w^{exp}||_{\mathbb{B}}^2} \quad , \tag{8}$$

in which $||g||_{\mathbb{B}}^2 \;=\; \displaystyle\int_{\mathbb{B}}|g(\omega)|^2\,d\omega$. The second cost function is written as

$$\underline{j}_{pha}(\mathbf{r}) \;=\; \frac{||\underline{\phi}_w(\mathbf{r},.) \;-\; \underline{\phi}_w^{exp}||_{\mathbb{B}}^2}{||\underline{\phi}_w^{exp}||_{\mathbb{B}}^2} \quad . \tag{9}$$

The updating of the mean computational model is then performed by solving the optimization problem:

$$\text{find } \mathbf{r}^{mod}\in\mathcal{R} \text{ such that } \underline{j}_{mod}(\mathbf{r}^{mod}) \le \underline{j}_{mod}(\mathbf{r}) \text{ for all } \mathbf{r}\in\mathcal{R} \quad ,$$

for the first cost function or the following one for the second cost function

$$\text{find } \mathbf{r}^{pha}\in\mathcal{R} \text{ such that } \underline{j}_{pha}(\mathbf{r}^{pha}) \le \underline{j}_{pha}(\mathbf{r}) \text{ for all } \mathbf{r}\in\mathcal{R} \quad .$$

Each constrained optimization problem can be solved numerically by using the sequential quadratic optimization algorithm [30,31]. Moreover, it should be noted that the gradient and the Hessian of cost functions $\underline{j}_{mod}(\mathbf{r})$ and $\underline{j}_{pha}(\mathbf{r})$ can easily be algebraically constructed.

Let $\mathbf{r}^{ini} \;=\; \{\xi_0^{ini},\xi_1^{ini},\alpha^{ini},\beta^{ini}\}$ for which $\xi_0^{ini} \;=\; \xi_1^{ini} \;=\; 0.01$, $\alpha^{ini} \;=\; 10$ and $\beta^{ini} \;=\; 42.84$ be the value of the updating mean parameter used for the initialization of the optimization algo-

rithm. In this case, since $\xi_0^{ini} = \xi_1^{ini}$, the modal damping model does not depend on parameters α^{ini} and β^{ini} (see Eq. 5). Such an initial value corresponds to a mean damping model for which the critical damping rate is constant over the low- and medium-frequency range and is equal to 0.01. The corresponding mean computational model is the mean computational model issued from the updating of the conservative parameters [23,25] and is in the present case the initial mean computational model. Moreover, since updating parameters α and β allows the position of the inflection point of function $b \mapsto f(b, \mathbf{r})$ to be controlled as soon as $\xi_0 < \xi_1$, the values $\alpha^{ini} = 10$ and $\beta^{ini} = 42.84$ are chosen in order to set the location of the initial inflection point at frequency $\nu = 3000\,Hz$.

3.5 Numerical Results

First, a convergence analysis is performed with respect to the reduced order model N. The convergence analysis is performed by analyzing the function $N \mapsto 10\,log_{10}\left(||\underline{\mathbf{w}}||^2_{\mathbb{B}}\right)$. Since updating parameters only concern damping, convergence with respect to N weakly depends on $\mathbf{r}$ and can be neglected in the convergence analysis. It has been verified that convergence is reached for $N = 120$. Figure 6 compares the graph of $\nu \mapsto \underline{dB}_w(\nu, \mathbf{r}^{ini})$ with $\nu \mapsto \underline{dB}_w^{exp}(\nu)$. Figures 7 compares the graph $\nu \mapsto \underline{\phi}_w(\nu, \mathbf{r}^{ini})$ with $\nu \mapsto \underline{\phi}_w^{exp}(\nu)$. It is seen that the quality of the initial mean computational model with respect to the experiments is quite good in the low-frequency range but has to be improved in the medium-frequency range.

The results obtained by solving the deterministic updating problem using the two cost functions $\underline{j}_{mod}(\mathbf{r})$ and $\underline{j}_{pha}(\mathbf{r})$ are then analyzed and discussed. The optimization of cost function $\underline{j}_{mod}(\mathbf{r})$ yields optimal updating mean parameters $\mathbf{r}^{mod} = \{0.0091, 0.1206, 10.6856, 46.2361\}$

whereas the optimization of cost function $\underline{j}_{pha}(\mathbf{r})$ yields optimal updating mean parameters $\mathbf{r}^{pha} = \{0.0099, 0.08495, 10.5867, 46.6657\}$. Figure 8 shows the graph $\nu \mapsto f(\nu, \mathbf{r}^{mod})$ and $\nu \mapsto f(\nu, \mathbf{r}^{pha})$ related to the two updated damping models. It is seen that the two cost functions yield similar function f in $[100\,,\,2000]\,Hz$ but are different for higher frequencies. In particular, it can be seen that the response of the updated mean computational model obtained with cost function $\underline{j}_{mod}(\mathbf{r})$ is more damped than the response of the updated mean computational model obtained with cost function $\underline{j}_{pha}(\mathbf{r})$.

Both optimization strategies are then compared (1) with respect to the initial mean computational model in order to quantify the improvement of the deterministic updating and (2) with respect to one to the other one in order to determine the best optimization strategy to be used in the present case. Figure 9 shows the graphs $\nu \mapsto \underline{dB}_w(\nu, \mathbf{r}^{mod})$, $\nu \mapsto \underline{dB}_w(\nu, \mathbf{r}^{pha})$ and $\nu \mapsto \underline{dB}_w^{exp}(\nu)$. Figure 10 shows the graph $\nu \mapsto \underline{\phi}_w(\nu, \mathbf{r}^{mod})$, $\nu \mapsto \underline{\phi}_w(\nu, \mathbf{r}^{pha})$ and $\nu \mapsto \underline{\phi}_w^{exp}(\nu)$. By comparing Figure 9 with Figure 6 and Figure 10 with Figure 7, it is seen that both cost functions yield an updated mean computational model which improves the updating in the medium-frequency range. Note that $\underline{j}_{mod}(\mathbf{r}^{mod}) = 0.3172\,\underline{j}_{mod}(\mathbf{r}^{ini})$ and $\underline{j}_{pha}(\mathbf{r}^{pha}) = 0.1821\,\underline{j}_{pha}(\mathbf{r}^{ini})$ which shows that this improvement is better using cost function $\underline{j}_{pha}(\mathbf{r})$ than with cost function $\underline{j}_{mod}(\mathbf{r})$. In Figure 9, it can be seen that the optimization of cost function $\underline{j}_{mod}(\mathbf{r})$ yields an updated mean computational model which matches relatively well with the experiment. Nevertheless, it should be noted that the dynamical behaviour of the sandwich panel is not well represented by this updated mean computational model in $[3000\,,\,4500]\,Hz$ because the mean computational model does not yield any resonance peakings in this frequency range. In Figure 10, it can be seen that the optimization of cost function $\underline{j}_{pha}(\mathbf{r})$ yields an updated mean computational model for which there is a good agreement with respect to the experiments in

both low and medium-frequency ranges.

Concerning the comparison of both optimization strategies with respect to the other, it should be noted that we have $\underline{j}_{mod}(\mathbf{r}^{pha}) = 0.4460\,\underline{j}_{mod}(\mathbf{r}^{ini})$ and $\underline{j}_{pha}(\mathbf{r}^{mod}) = 0.7755\,\underline{j}_{pha}(\mathbf{r}^{ini})$. Clearly, we have $\underline{j}_{mod}(\mathbf{r}^{mod}) < \underline{j}_{mod}(\mathbf{r}^{pha})$ and $\underline{j}_{pha}(\mathbf{r}^{pha}) < \underline{j}_{pha}(\mathbf{r}^{mod})$. These results show that cost function $\underline{j}_{pha}(\mathbf{r})$ is more sensitive to the updating mean parameters than cost function $\underline{j}_{mod}(\mathbf{r})$. In particular, by comparing Figures 9 and 10, one can see that $\mathbf{r}^{pha}$ is an updating point which is more acceptable for cost function $\underline{j}_{mod}(\mathbf{r})$ than $\mathbf{r}^{mod}$ is acceptable for cost function $\underline{j}_{pha}(\mathbf{r})$. All the comments above are related to the observations used in the cost function, which are global observations defined as a spatial average of the modulus or the phase of the frequency response functions. It is interesting to see the results on the physical observations which corresponds to the frequency response functions at the different measurment points. We are then interested in comparing the frequency response functions obtained by the two updated mean computational models with respect to the experimental frequency response functions. Let $\mathbf{m}_{\mathbb{w}}^{exp}(\omega) = (m_{\mathbb{w},1}^{exp}(\omega)), \ldots, m_{\mathbb{w},n_{obs}}^{exp}(\omega))$ be the $\mathbb{C}^{n_{obs}}$-vector such that $m_{\mathbb{w},j}^{exp}(\omega) = \dfrac{1}{n_{exp}} \displaystyle\sum_{k=1}^{n_{exp}} \mathbb{W}_j^{exp}(\omega, \theta_k)$ where $\mathbb{W}_j^{exp}(\omega, \theta_k) = 20\,log_{10}(|W_j^{exp}(\omega, \theta_k)|)$. Let $\underline{\mathbb{w}}_j(\mathbf{r}, \omega) = 20\,log_{10}(|\underline{w}_j(\mathbf{r}, \omega)|)$. Figures 11 and 12 show the graph of functions $\nu \mapsto \underline{\mathbb{w}}_i(\nu, \mathbf{r}^{mod})$, $\nu \mapsto \underline{\mathbb{w}}_i(\nu, \mathbf{r}^{pha})$ and $\nu \mapsto m_{\mathbb{w},i}^{exp}(\nu)$ in which the subscript $i = \{1, 2\}$ corresponds to observation point number i located at $\mathbf{x}_1 = (0.187, 0.047, 0)$ and $\mathbf{x}_2 = (0.037, 0.272, 0)$ (see Fig. 4. In Figures 11 and 12, it can be seen that both cost functions yield accurate results in the low-frequency band $[100\,,\,1200]Hz$ and yield satisfactory results in $[1200\,,\,3000]Hz$. In $[3000\,,\,4500]\,Hz$, it is clearly seen that the updated mean computational model obtained from cost function $\underline{j}_{pha}(\mathbf{r})$ yields a better agreement with respect to the experiment than the updated

mean computational model obtained from cost function $\underline{j}_{mod}(\mathbf{r})$.

Finally, from all these observations, it can then be deduced that cost function $\underline{j}_{pha}(\mathbf{r})$ is particularly adapted for solving this deterministic updating.

4 Robust updating method with respect to model uncertainties for the computational model of the dynamical system using the experimental frequency response functions

4.1 Description of the random matrix model

It is assumed that the mean computational model of the sandwich panel contains model uncertainties and data uncertainties. The probabilistic model used for modelling the uncertainties in the computational model is the non-parametric probabilistic approach. Below, the non-parametric probabilistic approach is briefly summarized.

The methodology of the non-parametric probabilistic approach consists of replacing matrices $[\underline{\mathcal{M}}]$, $[\underline{\mathcal{D}}(\mathbf{r})]$, $[\underline{\mathcal{K}}]$ by random matrices $[\boldsymbol{\mathcal{M}}]$, $[\boldsymbol{\mathcal{D}}(\mathbf{r})]$ and $[\boldsymbol{\mathcal{K}}]$ such that $\mathcal{E}\{[\boldsymbol{\mathcal{M}}]\} = [\underline{\mathcal{M}}]$, $\mathcal{E}\{[\boldsymbol{\mathcal{D}}(\mathbf{r})]\} = [\underline{\mathcal{D}}(\mathbf{r})]$ and $\mathcal{E}\{[\boldsymbol{\mathcal{K}}]\} = [\underline{\mathcal{K}}]$ in which $\mathcal{E}$ is the mathematical expectation and for which the probability distribution is known. The random matrices $[\boldsymbol{\mathcal{M}}]$, $[\boldsymbol{\mathcal{D}}(\mathbf{r})]$ and $[\boldsymbol{\mathcal{K}}]$ are written as $[\boldsymbol{\mathcal{M}}] = [\underline{L}_M]^T [\mathbf{G}_M] [\underline{L}_M]$, $[\boldsymbol{\mathcal{D}}(\mathbf{r})] = [\underline{L}_D(\mathbf{r})]^T [\mathbf{G}_D] [\underline{L}_D(\mathbf{r})]$ and $[\boldsymbol{\mathcal{K}}] = [\underline{L}_K]^T [\mathbf{G}_K] [\underline{L}_K]$ in which $[\underline{L}_M]$, $[\underline{L}_D(\mathbf{r})]$ and $[\underline{L}_K]$ are $N \times N$ real diagonal matrices such that $[\underline{\mathcal{M}}] = [\underline{L}_M]^T [\underline{L}_M]$, $[\underline{\mathcal{D}}(\mathbf{r})] = [\underline{L}_D(\mathbf{r})]^T [\underline{L}_D(\mathbf{r})]$ and $[\underline{\mathcal{K}}] = [\underline{L}_K]^T [\underline{L}_K]$ and where $[\mathbf{G}_M]$, $[\mathbf{G}_D]$ and $[\mathbf{G}_K]$ are full random matrices such that $\mathcal{E}\{|||[\mathbf{G}_M]|||_F\} = [I]$, $\mathcal{E}\{|||[\mathbf{G}_D]|||_F\} = [I]$, $\mathcal{E}\{|||[\mathbf{G}_K]|||_F\} = [I]$ and are with value in the set of all the positive-definite symmetric $N \times N$ matrices. The probability

model of random matrices $[\mathbf{G}_M]$, $[\mathbf{G}_D]$ and $[\mathbf{G}_K]$ is constructed by using the maximum entropy principle with the available information. All the details concerning the construction of this probability model can be found in [18,19,32]. The dispersion of each random matrix $[\mathbf{G}_M]$, $[\mathbf{G}_D]$ and $[\mathbf{G}_K]$ is controlled by one real positive parameter δ_M, δ_D and δ_K called the dispersion parameter. In addition, there exists an algebraic representation of this random matrix useful to the Monte Carlo numerical simulation. Let $\boldsymbol{\delta} = (\delta_M\,,\,\delta_D\,,\,\delta_K)$ be the $\mathbb{R}^3$-vector of the dispersion parameters defined on the admissible set $\mathcal{A} = \{[0\,,\,\sqrt{\frac{N+1}{N+5}}]\}^3$. It should be noted that the definition of admissible set $\mathcal{A}$ results from the construction of the probability model of matrix $[\mathbf{G}_M]$, $[\mathbf{G}_D]$ and $[\mathbf{G}_K]$ using the maximum entropy principle with the available information [18,19]. In coherence with the notation of Section 3.2, let $\mathbf{W}(\mathbf{r},\boldsymbol{\delta},\omega) = (W_1(\mathbf{r},\boldsymbol{\delta},\omega),\ldots,W_{n_{obs}}(\mathbf{r},\boldsymbol{\delta},\omega))$ be the $\mathbb{C}^{n_{obs}}$-valued random vector of the n_{obs} observations. The equations of the stochastic reduced matrix system constructed with the non-parametric approach of uncertainties are given by $\mathbf{W}(\mathbf{r},\boldsymbol{\delta},\omega) = [T(\omega)]\,[\underline{\Phi}]\,\mathbf{Q}(\mathbf{r},\boldsymbol{\delta},\omega)$, where $\mathbf{Q}(\mathbf{r},\boldsymbol{\delta},\omega)$ is the $\mathbb{C}^N$-valued random vector of the generalized coordinates, which is solution of the random matrix equation

$$\Big(-\omega^2\,[\boldsymbol{\mathcal{M}}] + i\,\omega\,[\boldsymbol{\mathcal{D}}(\mathbf{r})] + [\boldsymbol{\mathcal{K}}]\Big)\,\mathbf{Q}(\mathbf{r},\boldsymbol{\delta},\omega) = \underline{\boldsymbol{\mathcal{F}}}(\omega) \quad . \tag{10}$$

4.2 Formulation for the robust updating problem.

In this Section, the robust updating optimization problem is formulated. As explained in the Introduction, the cost function used for solving the robust updating problem is constructed with an uncertain computational model. The probabilistic model used for modelling the uncertainties in the computational model is the non-parametric probabilistic approach. With such a probabilistic approach, the probability model of random matrix $[\mathbf{G}_D]$ only depends on the dispersion param-

eter δ_D although the random matrix $[\boldsymbol{\mathcal{D}}(\mathbf{r})]$ does depend by construction on both dispersion parameter δ_D and mean updating parameter $\mathbf{r}$. Consequently, the cost function which describes the performance of the uncertain computational model with respect to the experimental measurements is a function of two classes of updating parameters : the updating mean parameter $\mathbf{r}$ and the updating dispersion parameter $\boldsymbol{\delta}$.

In this paper, the cost function proposed for the formulation of the robust updating problem. is denoted as $j(\mathbf{r}, \boldsymbol{\delta})$ and is defined as the sum of (1) the bias between the mean value of the uncertain computational model and the mean value of the experiment and (2) the variance of the uncertain computational model. Cost function $j(\mathbf{r}, \boldsymbol{\delta})$ is then written as

$$j(\mathbf{r}, \boldsymbol{\delta}) \;=\; \gamma \, ||\mathbf{m}_{\mathbb{W}}(\mathbf{r}, \boldsymbol{\delta}, \cdot) \;-\; \mathbf{m}_{\mathbb{W}}^{exp}||_{\mathbb{B}}^2 \;+\; (1-\gamma) \, |||\mathbb{W}(\mathbf{r}, \boldsymbol{\delta}, \cdot) \;-\; \mathbf{m}_{\mathbb{W}}(\mathbf{r}, \boldsymbol{\delta}, \cdot)|||^2 \quad , \qquad (11)$$

in which $\mathbf{m}_{\mathbb{W}}(\mathbf{r}, \boldsymbol{\delta}, \omega) \;=\; \mathcal{E}\{\mathbb{W}(\mathbf{r}, \boldsymbol{\delta}, \omega)\} \;\in\; \mathbb{C}^{n_{obs}}$, where $\mathbb{W}(\mathbf{r}, \boldsymbol{\delta}, \omega) \;=\; (\mathbb{W}_1(\mathbf{r}, \boldsymbol{\delta}, \omega), \ldots,$ $\mathbb{W}_{n_{obs}}(\mathbf{r}, \boldsymbol{\delta}, \omega))$ with $\mathbb{W}_j(\mathbf{r}, \boldsymbol{\delta}, \omega) \;=\; 20\, log_{10}(|W_j(\mathbf{r}, \boldsymbol{\delta}, \omega)|)$ and where $||\mathbf{g}||_{\mathbb{B}}^2 \;=\; \int_{\mathbb{B}} \, ||\mathbf{g}(\omega)||^2 \, d\omega$ with $||\mathbf{g}(\omega)||$ the Hermitian norm of $\mathbf{g}(\omega)$. In Eq. (11), the norm $|||\mathbb{X}|||$ is defined by $|||\mathbb{X}|||^2 \;=$ $E\{||\mathbb{X}||_{\mathbb{B}}^2\}$, where $\{\mathbb{X}(\omega), \omega \in \mathbb{B}\}$ is a stochastic process indexed by $\mathbb{B}$. Moreover, the scalar γ is a weighting factor belonging to $]0\,,\; 1[$ which allows the weight of the bias term with respect to the variance term in the optimization process to be quantified. It should be noted that cost function $j(\mathbf{r}, \boldsymbol{\delta})$ does not correspond to a direct generalization of Eq. (8). Indeed, the cost functions $\underline{j}_{mod}(\mathbf{r})$ and $\underline{j}_{pha}(\mathbf{r})$ are defined as a distance between two quantities which are averaged over the space variables. In the previous Section, it is shown that these cost functions are particularly adapted to the deterministic updating. However, its generalization for the robust updating does not allow the quality of the uncertain computational model with respect to the experiments to be accurately quantified. Indeed, such a generalization would yield a cost function defined by

a norm describing a distance between two quantities spatially and statistically averaged. The combination of these two types of averaging does not yield any satisfactory results because the variability induced by the randomness can not be distinguished from one observation point to another one. Such a norm is then too rough and is not appropriated in the context of robust updating. Consequently, a more refined norm is introduced in Eq. (11). For each observation point, this norm is related to the square integrable norm over the low- and medium- frequency range and describes for each observation point the quality of the uncertain computational model with respect to the experiments. The robust updating problem leads to a non-linear constrained optimization problem which consists in minimizing the cost function with respect to the admissible set $\mathcal{R} \times \mathcal{A}$. The robust updating problem consists in solving the optimization problem

$$\text{find } (\mathbf{r}^{RU}, \boldsymbol{\delta}^{RU}) \in \{\mathcal{R} \times \mathcal{A}\} \text{ such that } j(\mathbf{r}^{RU}, \boldsymbol{\delta}^{RU}) \leq j(\mathbf{r}, \boldsymbol{\delta}) \quad , \quad \forall (\mathbf{r}, \boldsymbol{\delta}) \in \{\mathcal{R} \times \mathcal{A}\}.$$

4.3 Numerical aspects

The robust updating process concerning the optimization of cost function $j(\mathbf{r}, \boldsymbol{\delta})$ is described as follows. First, the updating mean parameter $\mathbf{r}^{pha}$ calculated in the previous Section is used as the initial updating mean parameter $\mathbf{r}^0$ for the robust updating optimization problem. One then has $\mathbf{r}^0 = \mathbf{r}^{pha}$. Secondly, the initial updating dispersion parameter $\boldsymbol{\delta}^0$ is calculated by minimizing cost function $j(\mathbf{r}^0, \boldsymbol{\delta})$ with respect to the admissible set $\mathcal{A}$. Since the cost function is not convex, such a constrained optimization problem is solved by using a genetic algorithm [33] coupled with the Monte Carlo numerical simulation. Thirdly, in order to refine the optimum, one solves the robust design optimization problem around updating parameters $(\mathbf{r}^0, \boldsymbol{\delta}^0)$. The cost function $j(\mathbf{r}, \boldsymbol{\delta})$ is then minimized with respect to the admissible set of updating parameters $\mathcal{R} \times \mathcal{A}$ by

using the sequential quadratic optimization algorithm [30,31,34] coupled with the Monte Carlo numerical simulation.

4.4 Numerical results

First, a convergence analysis is performed with respect to the number N of eigenmodes and the number n_s of realizations for the Monte Carlo numerical simulation. A convergence analysis is carried out for updating parameters $\mathbf{r} = (0.01, 0.01, \alpha, \beta)$ and $\boldsymbol{\delta} = (0.23, 0.43, 0.25)$. Such an analysis shows that convergence is reasonably reached for $n_s = 750$ and $N = 300$. One then presents the optimization of cost function $j(\mathbf{r}, \boldsymbol{\delta})$ with respect to the admissible set $\mathcal{R} \times \mathcal{A}$ for a weighting factor $\gamma = 0.25$. It should be noted that cost function $j(\mathbf{r}, \boldsymbol{\delta})$ is a multiobjective function for which the variance term describes the width of the confidence region obtained from the uncertain computational model. Any value γ belonging to $]0, 0.5[$ means that more importance is attributed in the minimization of the width of the confidence region. The value $\gamma = 0.5$ corresponds to the natural case for which each objective is equally considered. Any value γ belonging to $]0.5, 1[$ is obsolete in the present context because it is expected that the experimental data is included in a small confidence region. In this work, two values of γ have been tried : $\gamma = 0.5$ and $\gamma = 0.25$. The best result is found to be for $\gamma = 0.25$. For this value, the experimental data is included in the confidence region of the updated computational model. The initial updating parameters used for initializing the robust updating are first calculated and yield $\mathbf{r}^0 = \mathbf{r}^{pha} = (0.0099, 0.08495, 10.5867, 46.6657)$ and $\boldsymbol{\delta}^0 = (0.30, 0.19, 0.09)$. Note that the cost function is normalized such that $j(\mathbf{r}^0, \boldsymbol{\delta}^0) = 1$. The optimization of cost function $j(\mathbf{r}, \boldsymbol{\delta})$ with respect to the admissible set $\mathcal{R} \times \mathcal{A}$ yields optimal updating parameters

$\mathbf{r}^{RU} = (0.01, 0.0850, 10.7144, 46.1018)$ and $\boldsymbol{\delta}^{RU} = (0.31, 0.20, 0.14)$ which corresponds to $j(\mathbf{r}^{RU}, \boldsymbol{\delta}^{RU}) = 0.8248$. Figure 13 shows the graph $\nu \mapsto f(\nu, \mathbf{r}^0)$ and $\nu \mapsto f(\nu, \mathbf{r}^{RU})$ in order to compare the damping model of the structure corresponding to the deterministic updating and to the robust updating. In particular, it can be seen that both damping models are comparable in the frequency band $[100\,,\,2000]\,Hz$ and that the updated mean computational model is more damped when frequency increases. Figures 14 to 19 compare the experiments with the confidence region of the random response $\mathbb{W}_i(\mathbf{r}^{RU}, \boldsymbol{\delta}^{RU}, \nu)$ for $i = \{1, 2, 3, 4, 5, 6\}$ obtained with a probability level $P_c = 0.96$. The subscript $i = \{1, 2, 3, 4, 5, 6\}$ corresponds to the observation point number i located at points $\mathbf{x}_1 = (0.187, 0.047, 0)$, $\mathbf{x}_2 = (0.037, 0.272, 0)$, $\mathbf{x}_3 = (0.037, 0.047, 0)$, $\mathbf{x}_4 = (0.037, 0.159, 0)$, $\mathbf{x}_5 = (0.112, 0.159, 0)$, $\mathbf{x}_6 = (0.037, 0.215, 0)$ see Fig. 4. These figures show that there is a good agreement between the experiments and the updated computational model in both low- and medium-frequency ranges. In particular, it can be seen on figures 18 and 19 that the updated computational model matches well with the experiments in both low- and medium-frequency ranges.

It should be noted that some discrepancies between the experiments and the confidence region related to the updated uncertain computational model can be locally observed. These discrepancies are mainly explained by the fact that the confidence region of the uncertain computational model is calculated with a probability level of 0.96. In Figures 17 and 18, it can be seen that all the experiments are outside the confidence region in frequency band $[2800\,,\,3000]$ Hz. Clearly, small increasing of dispersion parameter $\boldsymbol{\delta}$ will lead the experiments to belong to the confidence region. However, the choice of the cost function defined in terms of the bias and variance yields this global minimum. This aspects could be improved in substituting this cost function by

another one imposing the experiments to be inside the confidence region. Such a cost function corresponds to a non-differentiable cost function [35]. Presently, for computational reasons, one has preferred to use a differentiable cost function in order to decrease the numerical costs.

Concerning the quantification of the robustness of the updated uncertain computational model, it is recalled that cost function defined by Eq. (11) provides a robustness measure of the updating. First, the cost function has been defined from an uncertain computational model which has been constructed with a non-parametric probabilistic approach. This means that robustness is understood as robustness with respect to model uncertainties and to data uncertainties. Secondly, the robustness of the uncertain computational model is quantified by the width of the confidence region which has to include the experimental measurments. If the confidence region is broad, this means that the uncertain computational model is sensitive to both model and data uncertainties and the robustness of the uncertain computational model is poor. On the contrary, if the confidence region is narrow, this means that the updated uncertain computational model is robust with respect to model uncertainties and data uncertainties. With regard to this analysis, it can be seen on figures 14 to 19 that the confidence region is narrow in the low-frequency band $\mathbb{B}_L = [100\,,\,1200]\,Hz$ which means that the updated computational model is robust with respect to data and model uncertainties in $\mathbb{B}_L$. The higher the frequency is, the broader the confidence region is. This means that this robustness decreases in the medium-frequency range $\mathbb{B}_M = [1200\,,\,4500]\,Hz$. Moreover, it should be noted that there exist local sub-frequency band in the medium-frequency range for which the confidence region of the updated computational model is relatively narrow. For example, it can be seen on figure 18 that for observation point $\mathbf{x}_5$, the updated computational model is more robust with respect to data and model uncertainties in $[3000\,,\,3500]\,Hz$ and in $[4000\,,\,4500]Hz$ than in $[3500\,,\,4000]\,Hz$.

5 CONCLUSIONS

In the present paper, a methodology has been proposed for the robust updating problem in the context of structural dynamics with uncertainties in the low- and medium-frequency ranges. The objective is not the updating of the mean computational model but the robust updating of the uncertain computational model which is considered as the predictive model. This methodology is validated from experimental results issued from a set of 8 manufactured composite sandwich panels. Concerning the first deterministic updating of the mean computational model (no uncertainties in the dynamical system), it is shown that the use of a cost function defined with the unwrapped phase of frequency response functions is particularly adapted. Concerning the second robust updating with respect to data and model uncertainties (using a stochastic computational model), it is shown that the methodology yields an updated uncertain computational model which is in good agreement with the experiments in the low- and medium-frequency ranges.

6 ACKNOWLEDGEMENTS

The authors thank the Laboratoire d'Analyse des Matériaux et Identification (LAMI) of the Ecole Nationale des Ponts et Chaussées for providing the experimental protocol. The authors gratefully acknowledge C. Chen for performing the experimental measurements. Finally, the authors thank the French Research National Agency for supporting this research (ANR CORODYNA project number NT05-2-41776).

References

[1] H. Berger, L. Barthe, R. Ohayon, Parametric updating of a finite element model from experimental modal characteristics, Mechanical Systems and Signal Processing 4 (3) (1990) 233–242.

[2] P. Ladeveze, M. Reynier, H. Berger, R. Ohayon, F. Quetin, L. Barthe, Updating methods of dynamic structured finite element model: dynamic reaction forces approach and error in constitutive equation approach, La Recherche Aérospatiale 5 (1991) 9–20.

[3] C. Farhat, F. Hemez, Updating finite element dynamic models using an element-by-element sensitivity methodology, AIAA Journal 31 (9) (1993) 1702–1711.

[4] J. Mottershead, M. Friswell, Model updating in structural dynamics : a survey, Journal of Sound and Vibration 167 (1993) 347–375.

[5] R. Levin, N. Lieven, Dynamic finite element model updating using neural networks, Journal of Sound and Vibration 210 (5) (1998) 593–607.

[6] P. Ladeveze, A. Chouaki, Application of a posteriori error estimation for structural model updating, Inverse Problem 15 (1999) 49–58.

[7] W. D'Ambrogio, A. Fregolent, The use of antiresonances for robust model updating., Journal of Sound and Vibration 236 (2) (2000) 227–243.

[8] F. Hemez, S. Doebling, Review and assessment of model updating for non linear transient dynamics, Mechanical Systems and Signal Processing 15 (1) (2001) 45–74.

[9] J. Raynaud, N. Bouhaddi, A. Perriot, Updating complex structures by a robust multilevel condensation approach., Journal of Sound and Vibration 270 (1-2) (2004) 403–416.

[10] B. Jaishi, R. Wei-Xin, Damage detection by finite element model updating using modal flexibility residual, Journal of Sound and Vibration 290 (2006) 369–387.

[11] K. Kwon, R. Lin, Robust finite element model updating using taguchi method, Journal of Sound and Vibration 280 (1-2) (2005) 77–99.

[12] C. Papadimitriou, J. Beck, L. Katafygiotis, Updating robust reliability using structural test data., Probabilistic Engineering Mechanics 16 (2) (2001) 103–113.

[13] C. Mares, J. Mottershead, M. Friswell, Stochastic model updating: Part 1 - theory and simulated example, Mechanical Systems and Signal Processing 20 (2006) 1674–1695.

[14] J. Mottershead, C. Mares, S. James, M. Friswell, Stochastic model updating: Part 1 - application to a set of physical structures, Mechanical Systems and Signal Processing 20 (2006) 2171–2185.

[15] H. Beyer, B. Sendhoff, Robust optimization - a comprehensive survey, Computer Methods in Applied Mechanics and Engineering 196 (2007) 3190–3218.

[16] E. Capiez-Lernout, C. Soize, Robust design optimization in computational mechanics, ASME Journal of Applied Mechanics, to appear in March 2008.

[17] E. Capiez-Lernout, C. Soize, Design optimization with an uncertain vibroacoustic model, ASME Journal of Vibration and Acoustics, to appear in 2008.

[18] C. Soize, A nonparametric model of random uncertainties for reduced matrix models in structural dynamics, Probabilistic Engineering Mechanics 15 (3) (2000) 277–294.

[19] C. Soize, A comprehensive overview of a non-parametric probabilistic approach of model uncertainties for predictive models in structural dynamics, Journal of Sound and Vibration 288 (3) (2005) 623–652.

[20] H. Chebli, C. Soize, Experimental validation of a nonparametric probabilistic model of nonhomogeneous uncertainties for dynamical systems, Journal of the Acoustical Society of America 115 (2) (2004) 697–705.

[21] E. Capiez-Lernout, C. Soize, J.-P. Lombard, C. Dupont, E. Seinturier, Blade manufacturing tolerances definition for a mistuned industrial bladed disk, ASME Journal of Engineering for Gas Turbines and Power 127 (3) (2005) 621–628.

[22] E. Capiez-Lernout, M. Pellissetti, H. Pradlwarter, G. Schueller, C. Soize, Data and model uncertainties in complex aerospace engineering systems, Journal of Sound and Vibration 295 (3-5) (2006) 923–938.

[23] C. Chen, D. Duhamel, C. Soize, Probabilistic approach for model and data uncertainties and its experimental identification in structural dynamics: case of composite sandwich panels, Journal of Sound and Vibration 294 (1-2) (2006) 64–81.

[24] J.-F. Durand, L. Gagliardini, C. Soize, Nonparametric modeling of the variability of vehicle vibroacoustic behavior, in: Proceedings on the SAE Noise and Vibration Conference and Exhibition, Traverse City, Michigan, USA, 16-19 May 2005, ISBN 0 7680 1657 6, 2005.

[25] C. Chen, Vibration et vibroacoustic of uncertain composite sandwich panels - experiments and model validation, phd thesis (in french), Ph.D. thesis (2006).

[26] R. Lyon, Range and frequency dependance of transfer function phase, Journal of the Acoustical Society of America 76 (5) (1984) 1433–1437.

[27] M. Tohyama, R. Lyon, Transfer function phase and truncated impulse response, Journal of the Acoustical Society of America 86 (5) (1989) 2025–2029.

[28] L. Wang, S. Walsh, Measurement of phase accumulation in the transfer functions of beams and plates, Journal of Sound and Vibration 290 (2006) 763–784.

[29] R. Ohayon, C. Soize, Structural acoustics and vibration, Academic Press, San Diego, London, 1998.

[30] M. Powell, Variable metric methods for constrained optimization, Mathematical Programming: the state of the art (1983) 288–311.

[31] R. Fletcher, Practical methods of optimization,constrained optimization (Vol.2), John Wiley and Sons, 1980.

[32] C. Soize, Random matrix theory for modeling random uncertainties in computational mechanics, Computer Methods in Applied Mechanics and Engineering 194 (12-16) (2005) 1333–1366.

[33] J. Spall, Introduction to stochastic search and optimization, Wiley Interscience, 2003.

[34] D. Luenberger, Optimization by vector space methods, Wiley Professional Paperback Series, 1969.

[35] C. Soize, E. Capiez-Lernout, J.-F. Durand, C. Fernandez, L. Gagliardini, Probabilistic model identification of uncertainties in computational models for dynamical systems and experimental validation., Computer Methods in Applied Mechanics and Engineering, submitted.

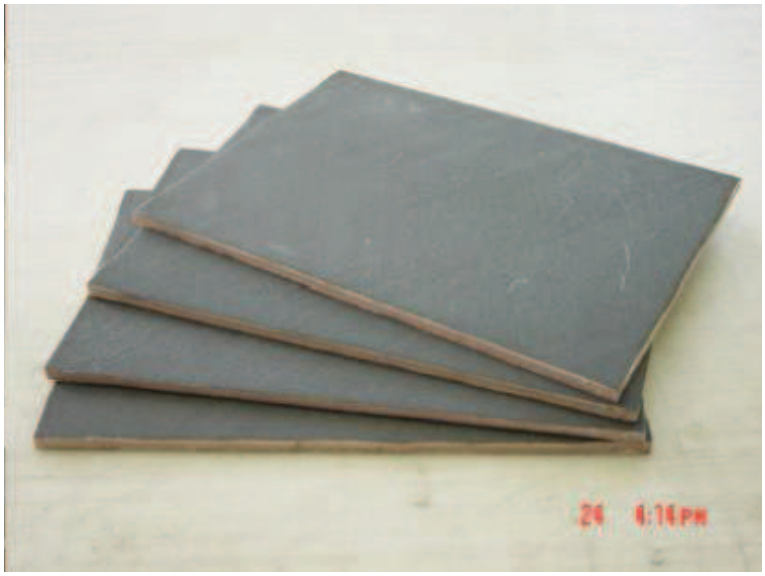

Fig. 1. Several samples of the sandwich panel

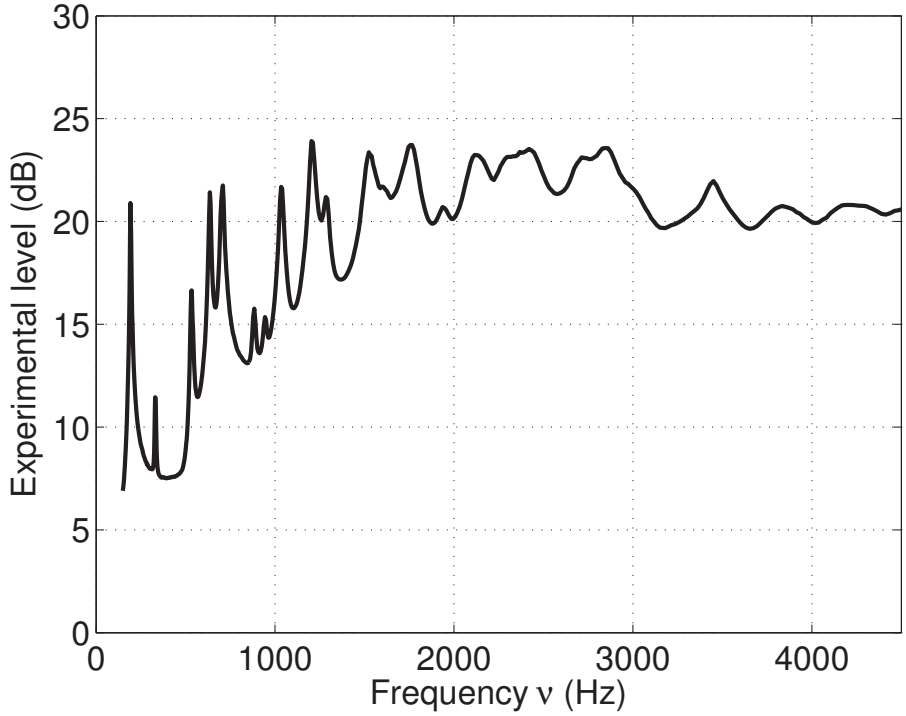

Fig. 2. Graph of the experimental averaged modulus $\nu \mapsto \underline{dB}_w^{exp}(\nu)$.

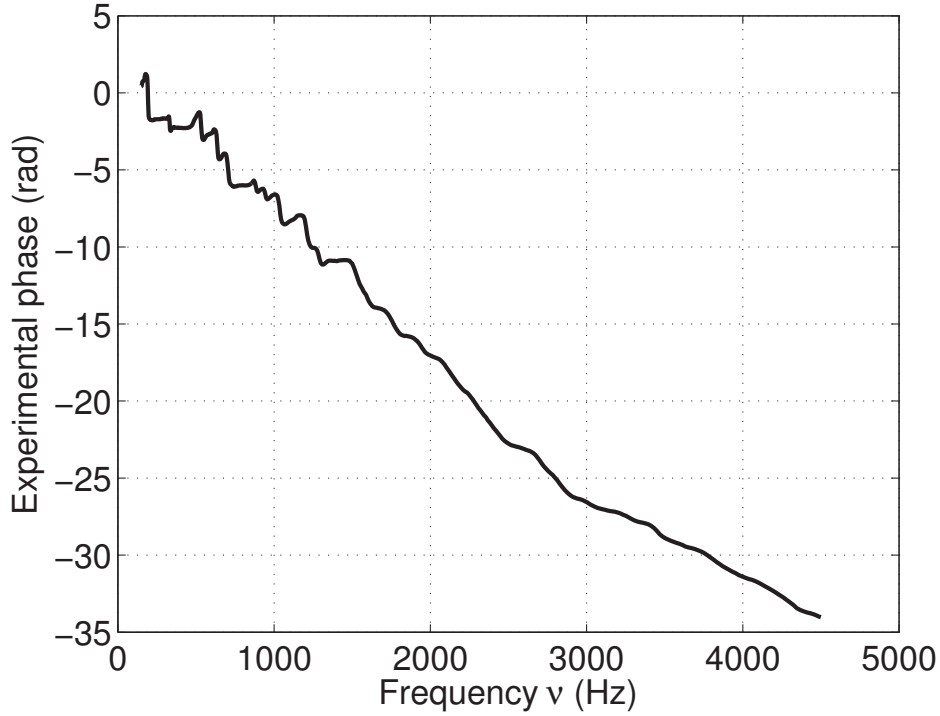

Fig. 3. Graph of the experimental averaged unwrapped phase $\nu \mapsto \underline{\phi}_w^{exp}(\nu)$.

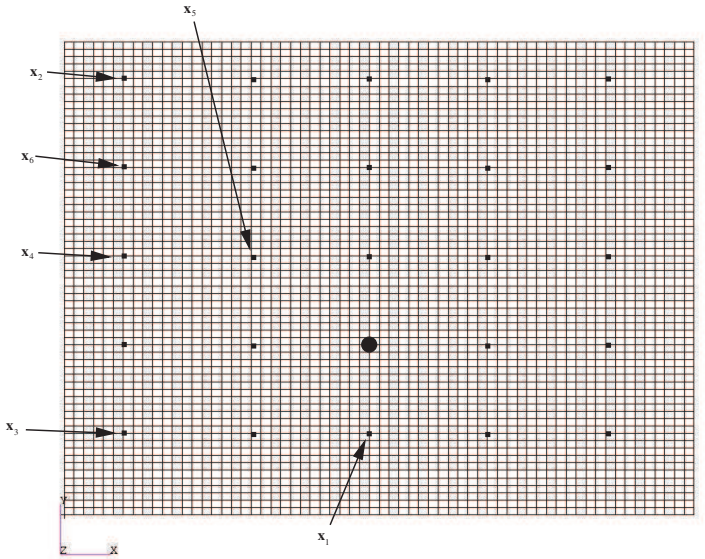

Fig. 4. Finite element mesh of the finite element model of the designed computational model - location of the measured observation points (black squares) - location of the excitation point (black circle).

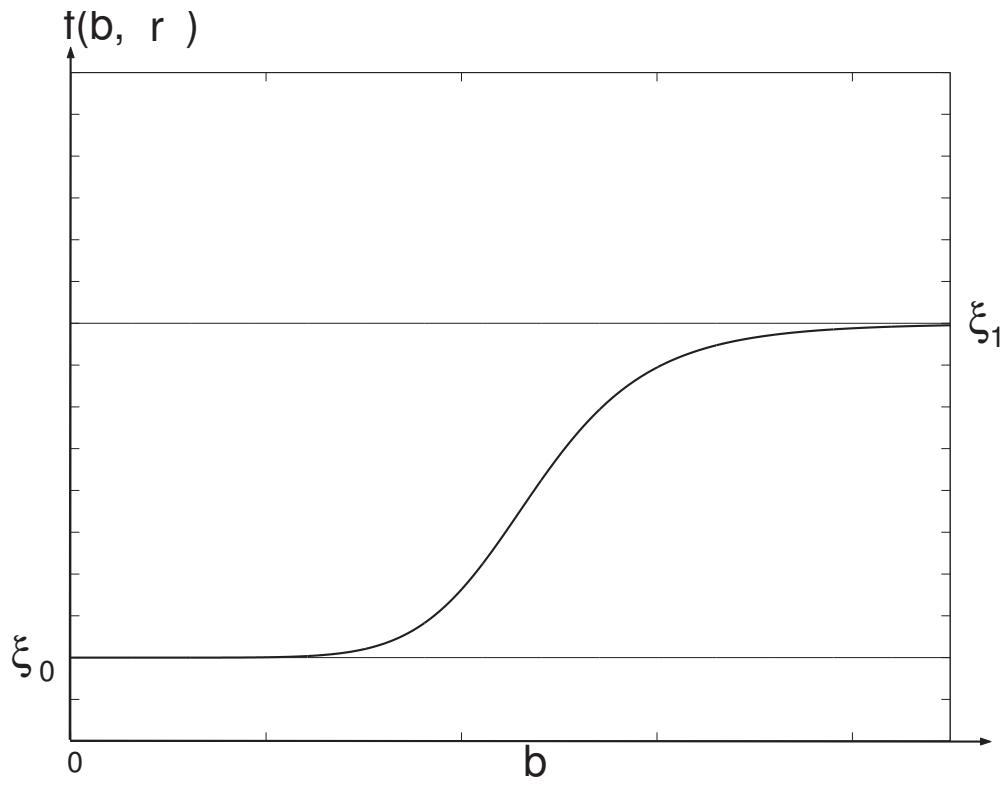

Fig. 5. Graph of function $b \mapsto f(b, \mathbf{r})$

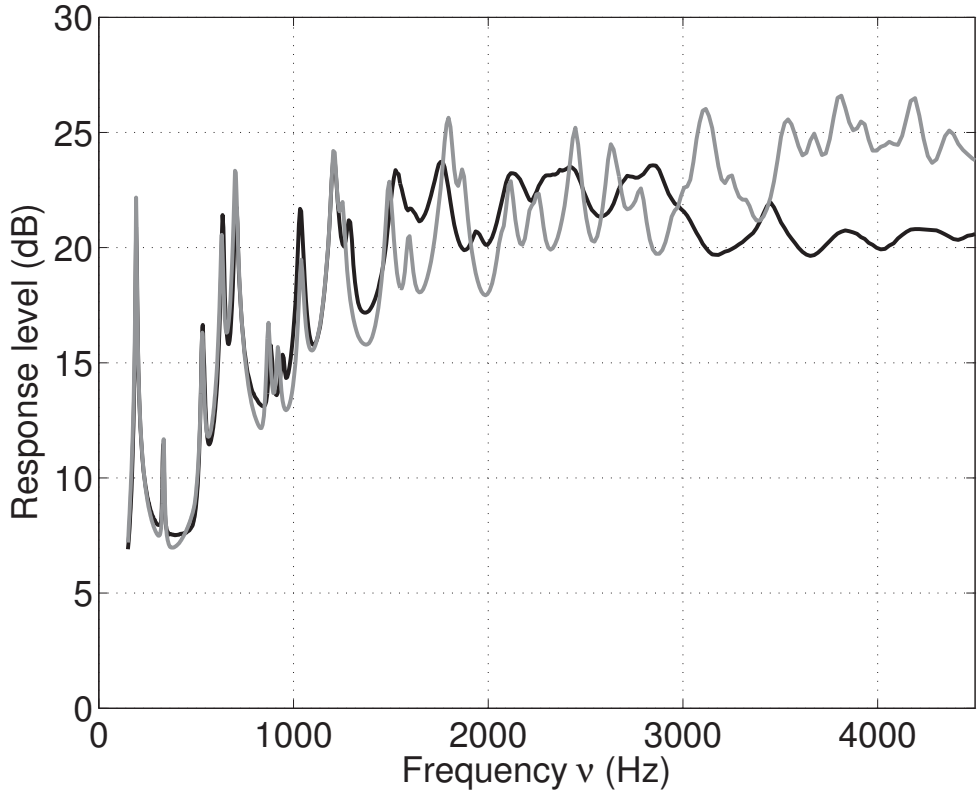

Fig. 6. Graph of function $\nu \mapsto \underline{dB}_w(\nu, \mathbf{r}^{ini})$ (thick gray line) and $\nu \mapsto \underline{dB}_w^{exp}(\nu)$ (thick black line)

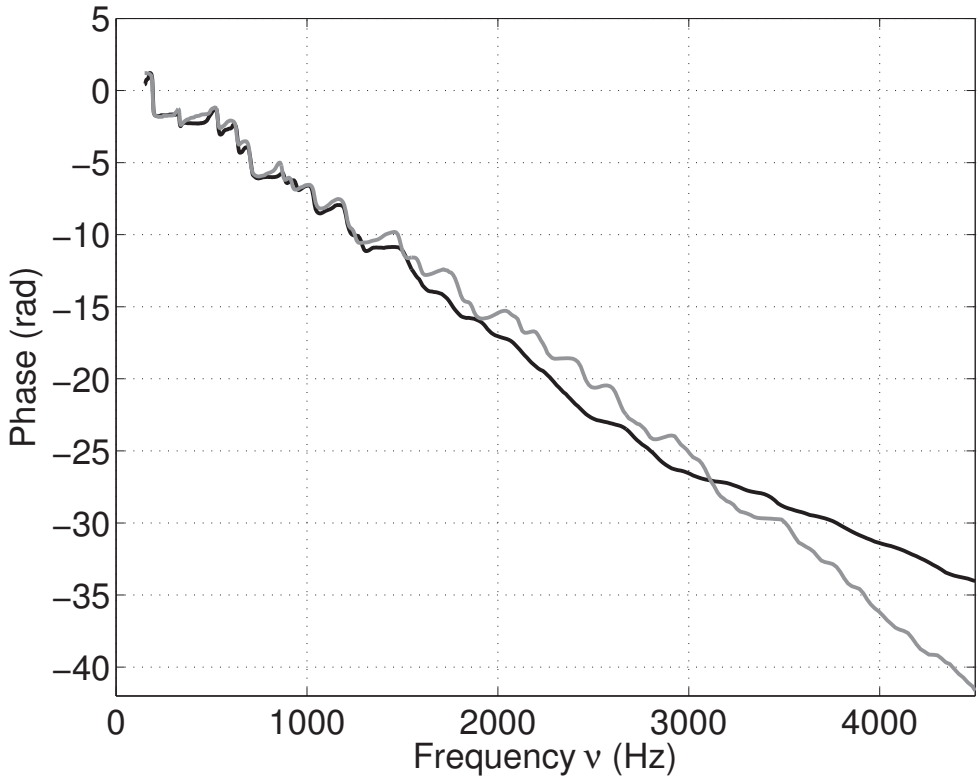

Fig. 7. Graph of function $\nu \mapsto \underline{\phi}_w(\nu, \mathbf{r}^{ini})$ (thick gray line) and $\nu \mapsto \underline{\phi}_w^{exp}(\nu)$ (thick black line)

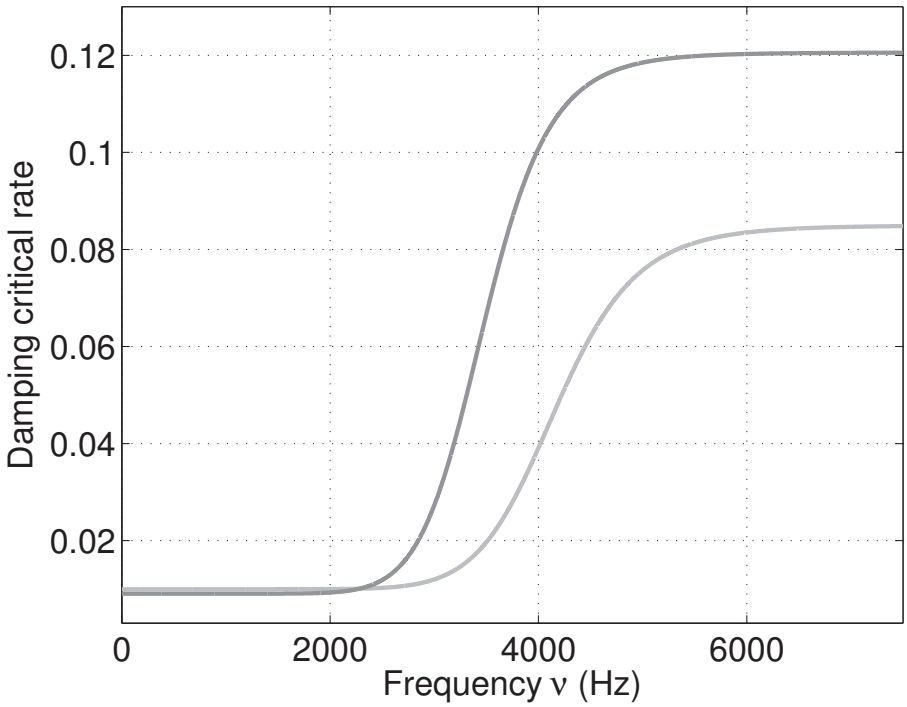

Fig. 8. (Graph of function $\nu \mapsto f(\nu, \mathbf{r}^{mod})$ (thick dark gray line) and $\nu \mapsto f(\nu, \mathbf{r}^{pha})$ (thick light gray line) corresponding to the updated mean damping model.

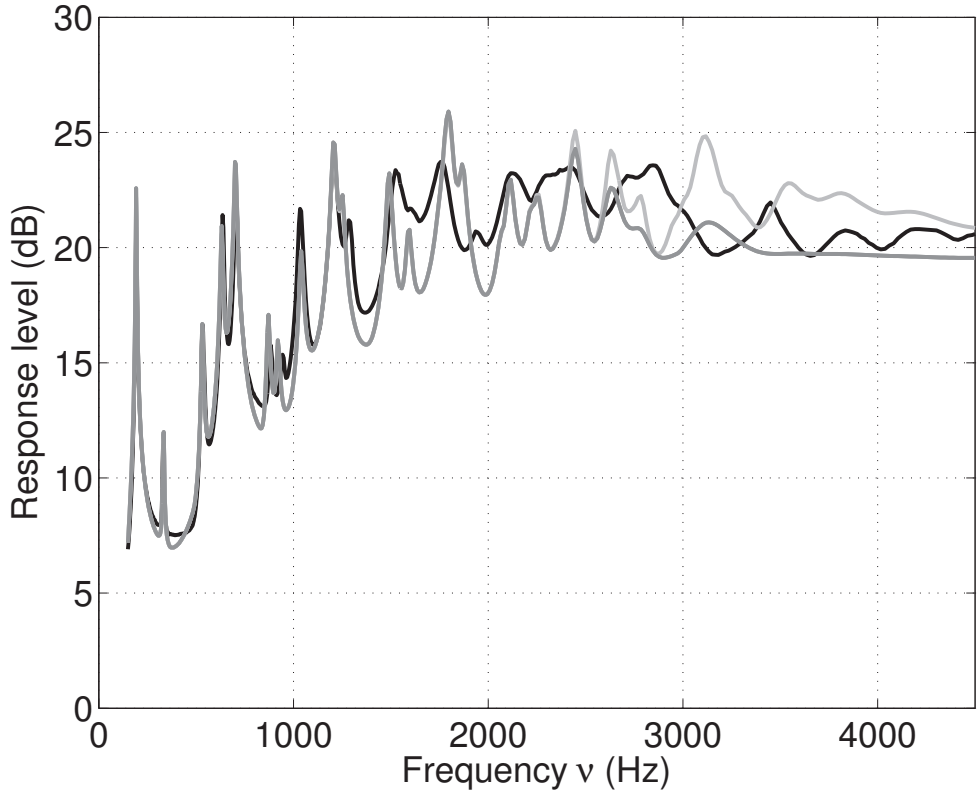

Fig. 9. Graph of function $\nu \mapsto \underline{dB}_w(\nu, \mathbf{r}^{mod})$ (thick dark gray line), $\nu \mapsto \underline{dB}_w(\nu, \mathbf{r}^{pha})$ (thick light gray line) and $\nu \mapsto \underline{dB}_w^{exp}(\nu)$ (thick black line).

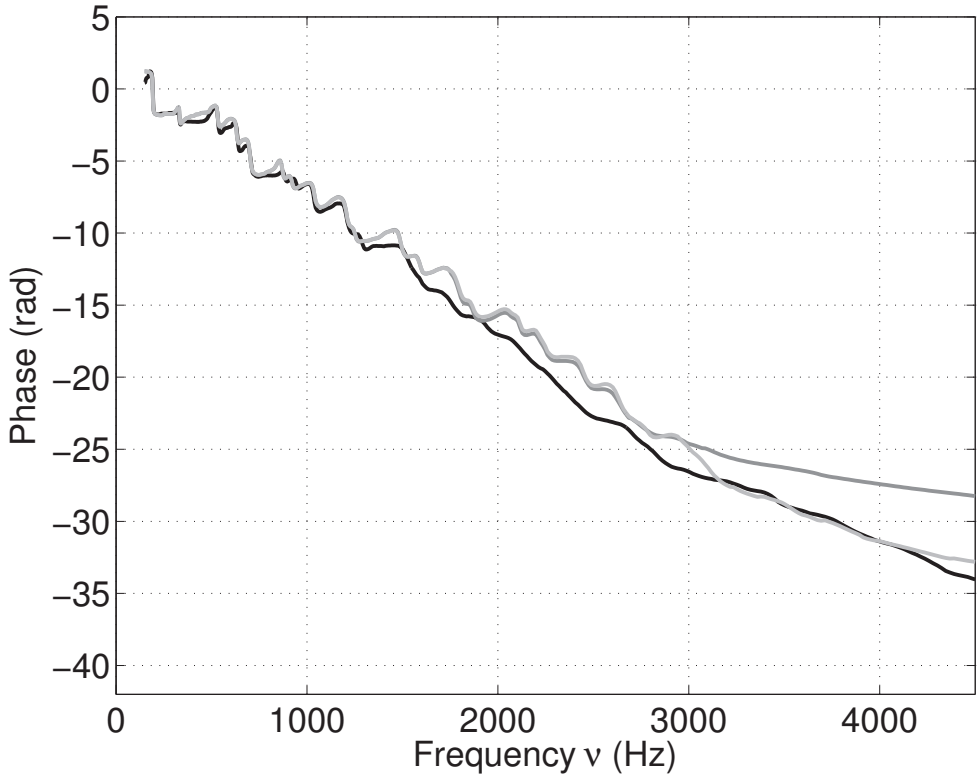

Fig. 10. Graph of function $\nu \mapsto \underline{\phi}_w(\nu, \mathbf{r}^{mod})$ (thick dark gray line), $\nu \mapsto \underline{\phi}_w(\nu, \mathbf{r}^{pha})$ (thick light gray line) and $\nu \mapsto \underline{\phi}_w^{exp}(\nu)$ (thick black line).

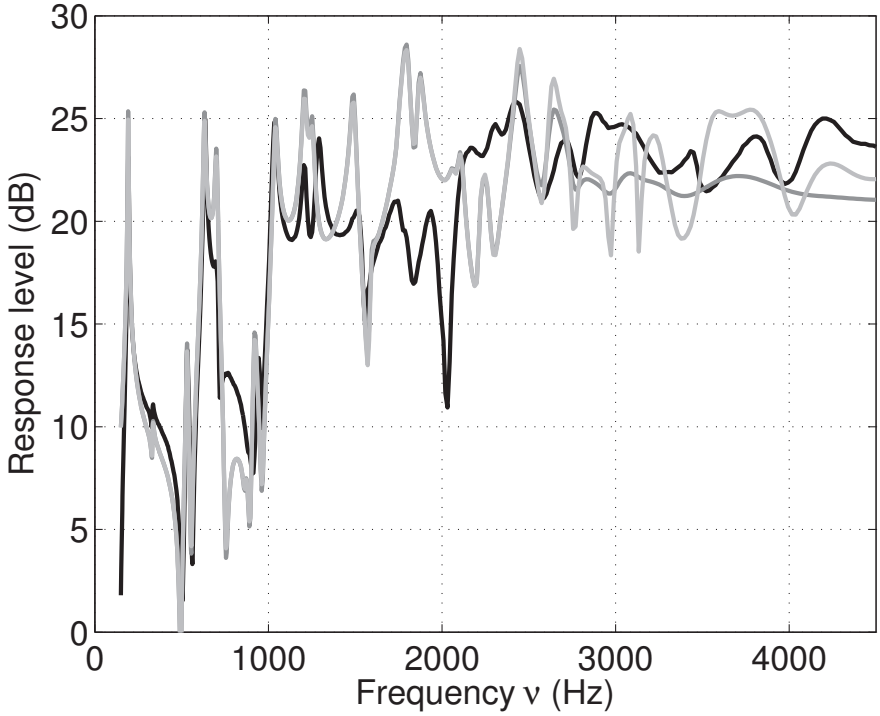

Fig. 11. Graph of $\nu \mapsto \underline{\mathbb{w}}_1(\nu, \mathbf{r}^{mod})$ (thick dark gray line), $\nu \mapsto \underline{\mathbb{w}}_1(\nu, \mathbf{r}^{pha})$ (thick light gray line) and $\nu \mapsto m^{exp}_{\mathbb{w},1}(\nu)$ (thick black line).

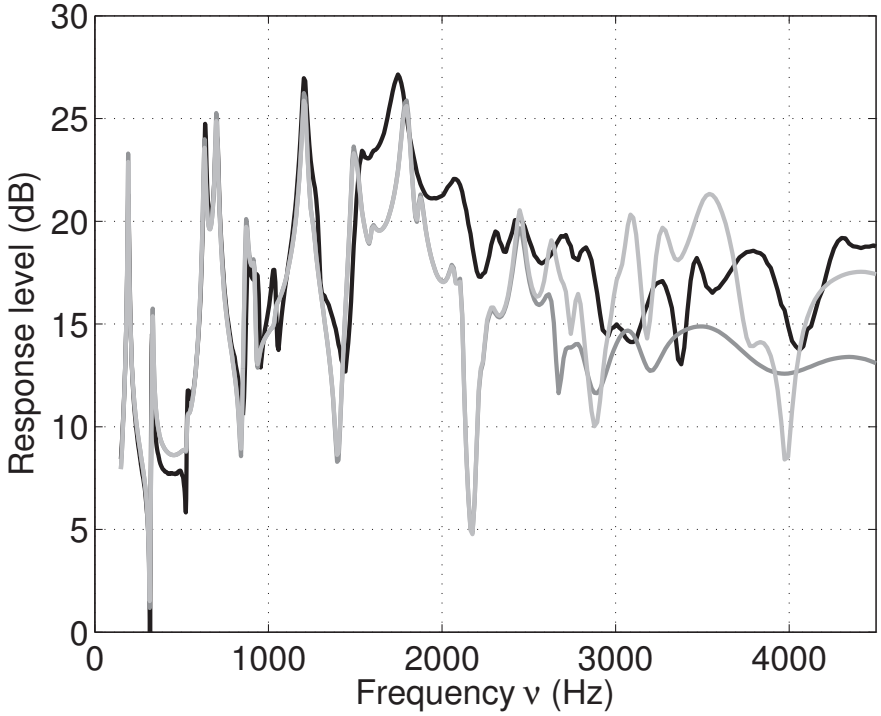

Fig. 12. Graph of $\nu \mapsto \underline{\mathbb{w}}_2(\nu, \mathbf{r}^{mod})$ (thick dark gray line), $\nu \mapsto \underline{\mathbb{w}}_2(\nu, \mathbf{r}^{pha})$ (thick light gray line) and $\nu \mapsto m^{exp}_{\mathbb{w},2}(\nu)$ (thick black line).

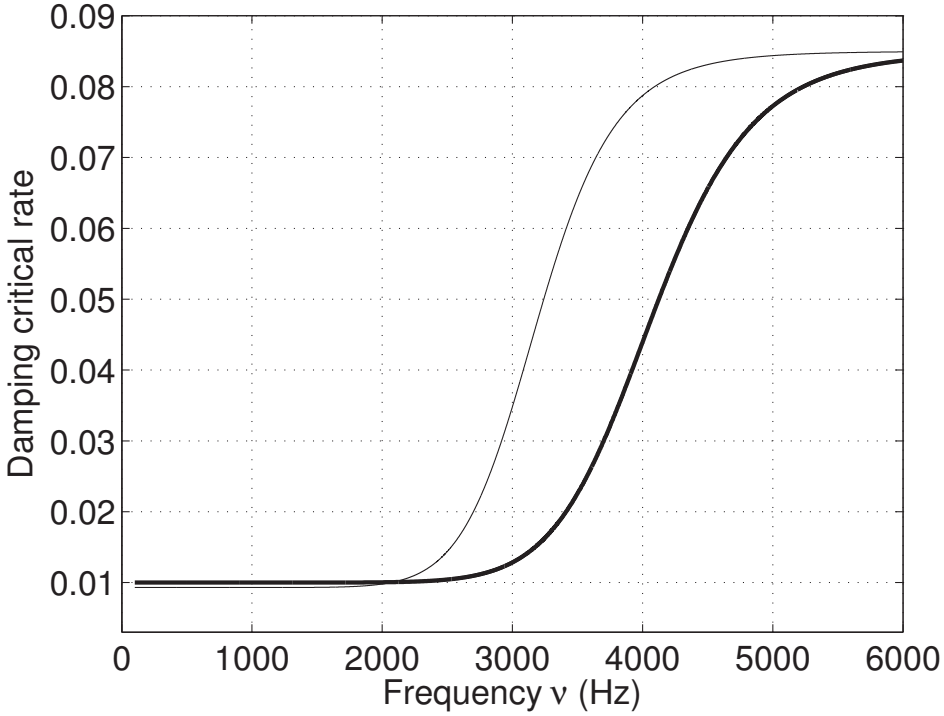

Fig. 13. Comparison between the damping model corresponding to the deterministic updating and to the robust updating. Graph of $\nu \mapsto f(\nu, \mathbf{r}^0)$ (thick line) and $\nu \mapsto f(\nu, \mathbf{r}^{RU})$ (thin line).

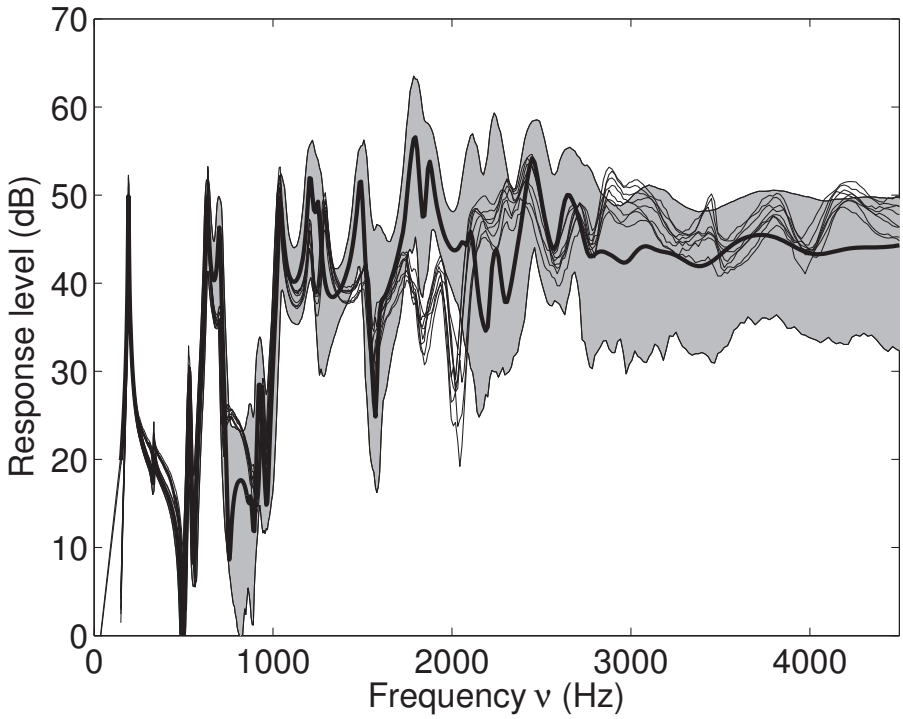

Fig. 14. Graph of $\nu \mapsto \mathbb{W}_1^{exp}(\nu, \theta_k)$ (thin black lines), graph of the confidence region of the random response $\nu \mapsto \mathbb{W}_1(\mathbf{r}^{RU}, \boldsymbol{\delta}^{RU}, \nu)$ (gray region), graph of $\nu \mapsto \underline{\mathbb{w}}_1(\mathbf{r}^{RU}, \nu)$ (thick black line).

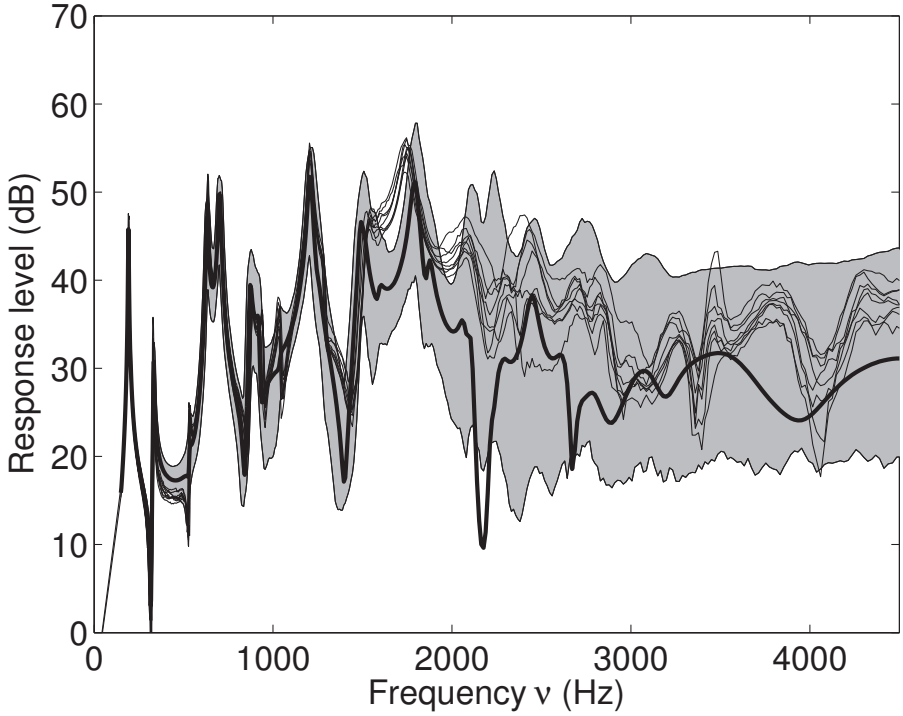

Fig. 15. Graph of $\nu \mapsto \mathbb{W}_2^{exp}(\nu, \theta_k)$ (thin black lines), graph of the confidence region of the random response $\nu \mapsto \mathbb{W}_2(\mathbf{r}^{RU}, \boldsymbol{\delta}^{RU}, \nu)$ (gray region), graph of $\nu \mapsto \underline{\mathbb{w}}_2(\mathbf{r}^{RU}, \nu)$ (thick black line).

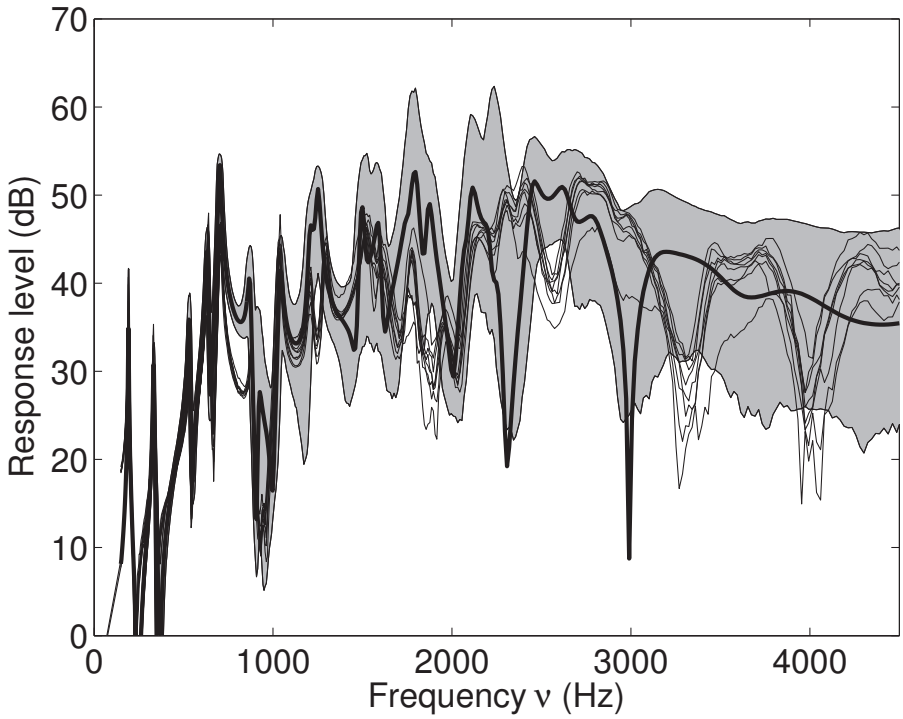

Fig. 16. Graph of $\nu \mapsto \mathbb{W}_3^{exp}(\nu, \theta_k)$ (thin black lines), graph of the confidence region of the random response $\nu \mapsto \mathbb{W}_3(\mathbf{r}^{RU}, \boldsymbol{\delta}^{RU}, \nu)$ (gray region), graph of $\nu \mapsto \underline{\mathbb{w}}_3(\mathbf{r}^{RU}, \nu)$ (thick black line).

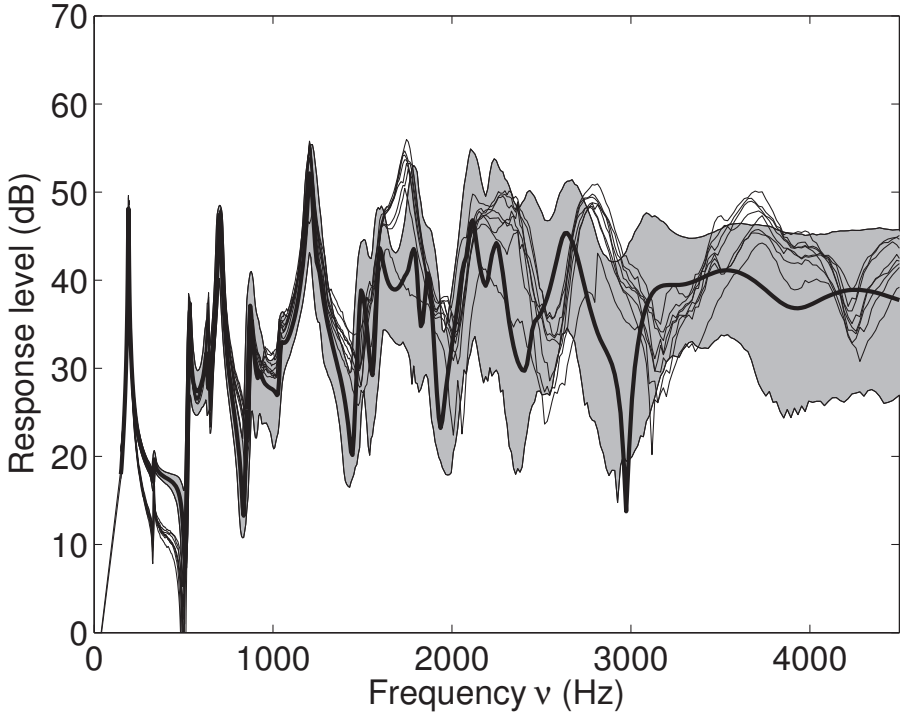

Fig. 17. Graph of $\nu \mapsto \mathbb{W}_4^{exp}(\nu, \theta_k)$ (thin black lines), graph of the confidence region of the random response $\nu \mapsto \mathbb{W}_4(\mathbf{r}^{RU}, \boldsymbol{\delta}^{RU}, \nu)$ (gray region), graph of $\nu \mapsto \underline{\mathbb{w}}_4(\mathbf{r}^{RU}, \nu)$ (thick black line).

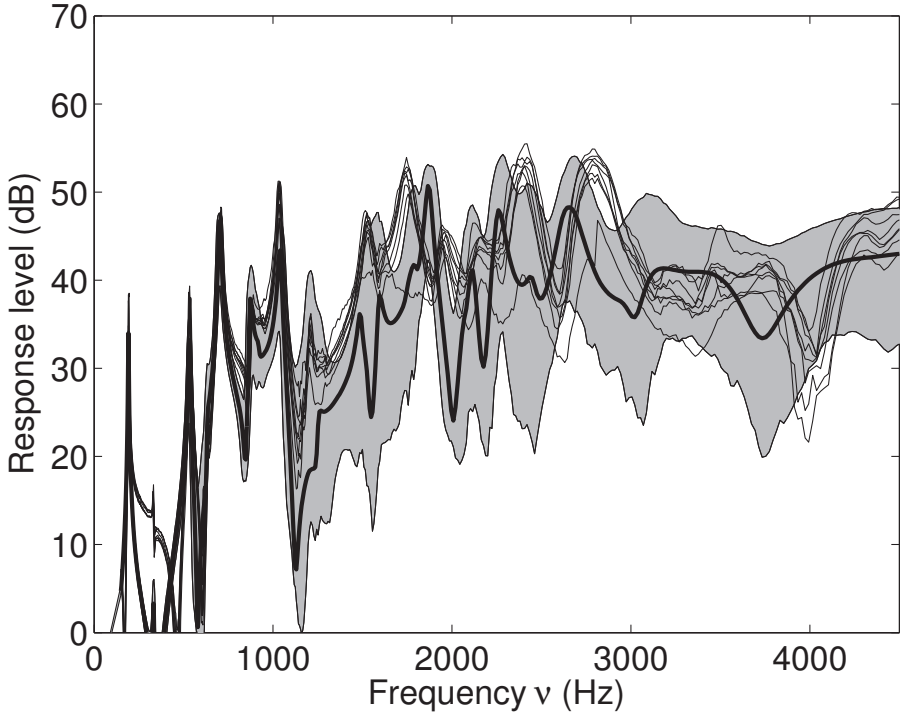

Fig. 18. Graph of $\nu \mapsto \mathbb{W}_5^{exp}(\nu, \theta_k)$ (thin black lines), graph of the confidence region of the random response $\nu \mapsto \mathbb{W}_5(\mathbf{r}^{RU}, \boldsymbol{\delta}^{RU}, \nu)$ (gray region), graph of $\nu \mapsto \underline{\mathbb{w}}_5(\mathbf{r}^{RU}, \nu)$ (thick black line).

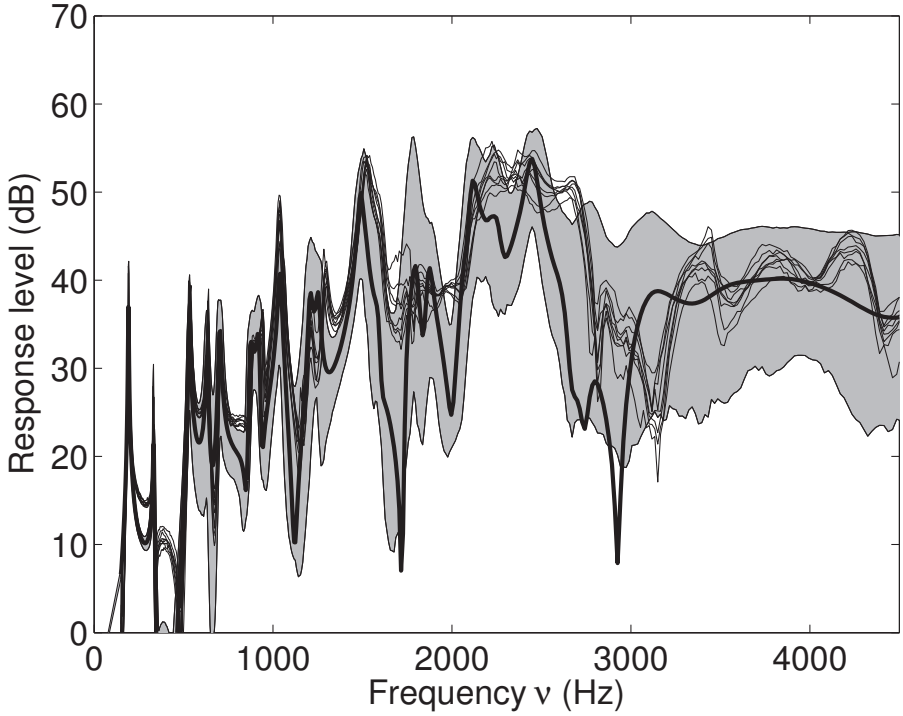

Fig. 19. Graph of $\nu \mapsto \mathbb{W}_6^{exp}(\nu, \theta_k)$ (thin black lines), graph of the confidence region of the random response $\nu \mapsto \mathbb{W}_6(\mathbf{r}^{RU}, \boldsymbol{\delta}^{RU}, \nu)$ (gray region), graph of $\nu \mapsto \underline{\mathbb{w}}_6(\mathbf{r}^{RU}, \nu)$ (thick black line).